# Prevention of Cooktop Ignition Using Detection and Multi-Step Machine Learning Algorithms

Wai Cheong Tam[a*], Eugene Yujun Fu[b*], Amy Mensch[a], Anthony Hamins[a*], Christina You[c], Grace Ngai[b], Hong va Leong[b]

[a]National Institute of Standards and Technology, 100 Bureau Dr., Gaithersburg, MD, USA, {waicheong.tam, amy.mensch, anthony.hamins}@nist.gov

[b]The Hong Kong Polytechnic University, 11 Yuk Choi Road, Kowloon, Hong Kong, China, {csyfu, csgngai, cshleong}@comp.polyu.edu.hk

[c]Carnegie Mellon University, 5000 Forbes Ave, Pittsburgh, PE, USA, cyou2@andrew.cmu.edu

*Corresponding author

## Highlights:

- Time series sensor data for cooking with electric-coil and gas cooktops are presented.
- Discussion of data preprocessing and feature selection for machine learning on real-time fire prevention application.
- Workflow for constructing and testing machine learning models is demonstrated.
- Support vector machine (SVM) detection algorithm correctly classifies 96.9 % of the data points as normal or hazardous conditions for oils on an electric-coil cooktop.
- Multi-step models can enhance data classification and improve overall detection accuracy.

## Abstract:

This paper[1] presents a study to examine the potential use of machine learning models to build a real-time detection algorithm for prevention of kitchen cooktop fires. Sixteen sets of time-dependent sensor signals were obtained from 60 normal or ignition cooking experiments. More than 200 000 data instances are documented and analyzed. The raw data are preprocessed. Selected features are generated for time series data focusing on real-time detection applications. Utilizing the leave-one-out cross validation method, three machine learning models are built and tested. Parametric studies are carried out to understand the diversity, volume, and tendency of the data. Given the current dataset, the detection algorithm based on support vector machine (SVM) provides the most reliable prediction of pre-ignition conditions (with an overall classification accuracy of 96.9 % for oils on an electric-coil cooktop). Analyses indicate that using a multi-step approach could further improve overall prediction accuracy. The development of an accurate detection algorithm can provide reliable feedback to intercept ignition of unattended cooking and help reduce fire losses.

**Keywords:** machine learning, time series classification, cooking, fire prevention, fire detection

[1] Certain commercial products are identified in this paper in order to specify adequately the equipment used. Such identification does not imply recommendation by the National Institute of Standards and Technology, nor does it imply that this equipment is the best available for the purpose.

## 1. Introduction

A study conducted by the National Fire Protection Association (NFPA) based on fire loss data from the National Fire Incident Reporting System summarizes the US cooking fire problem [1]. During the period 2013 – 2017, household fires involving cooking were responsible for approximately 173 200 fires, 5 020 injuries, and 550 deaths annually. This represents 49 % of all reported home fires in the US. In 2017, U.S. Fire Departments responded to an average of 470 home cooking fires per day. Of these fires, cooktops (or ranges) were found to be involved in 62 % of reported home cooking fire incidents, 89 % of home cooking fire deaths, and 79 % of home cooking fire injuries. Unattended cooking was the leading cause of cooking fires.

Households that use electric ranges have a higher risk of developing a cooking fire than those using gas ranges. Although 60 % of households cook with electric cooktops, 79 % of reported cooktop fires were electric [1]. In terms of standards development, the abnormal ignition test in UL 858[2] represents significant progress in addressing unattended electric-coil heating element cooktop fires [2]. However, there are no current analogous standards applicable to other types of electric cooktops or to gas ranges in North America, and there are no standards for existing electric-coil element cooktops/ranges manufactured before 2019. Additionally, the cooking fire problem in the US may be worse than it was a few decades ago. Cooking caused more home fire deaths in 2013-2017 than in 1980-1984 [1]. In summary, the cooking fire problem has not been adequately addressed and the consequent fire casualties. New approaches are needed to reduce cooking fires.

Typical smoke detectors being installed in kitchens are well-known to be prone to nuisance alarms caused by normal cooking activities. Despite research efforts made to understand the cooking fire characteristics [3,4], the signal behavior of various sensors [5,6] and the development of advanced cooking ignition detection algorithms [7,8], only a few of these improvements can be used in practical environments. Indeed, studies [9,10] show that commercially available smoke detectors are primarily designed to provide alerts and/or warnings for flaming fires in which fuel packages such as upholstered furniture, appliances, and/or kitchenware are being ignited. For detection of cooktop pre-ignition conditions, alterative detection technologies and analysis are needed.

Johnsson [11] conducted a series of experiments to determine the feasibility of using research-grade sensors to distinguish the signal behaviors between normal cooking activities and ignition conditions on an electric range in a mock kitchen. Optimal location for sensor placement and the associated cut-off value for such a detection system were suggested. More recently, Mensch et al. [12] extended the work of Johnsson using a wide range of consumer-grade sensors to develop a pre-ignition detection system. Sensor signal differences were investigated, and a threshold based on the magnitude of a volatile organic compounds (VOC) sensor was determined to best differentiate the signal peak for normal cooking and the minimum signal 60 s before ignition. More recently, the pre-ignition detection system was extended to account for both normal and ignition cooking conditions using gas cooktops [13]. Mensch and co-workers conducted a statistical analysis and showed that the previously determined threshold for the VOC sensor had to be modified to accommodate the additional data and to assure detection sensitivity and

[2] An “abnormal” ignition test was extended to consider the average temperature of a dry (without cooking oil), round, 20 cm diameter, cast iron pan [2]. If the average pan temperature does not exceed 385 °C for 30 min with the element on its highest power setting, the test is considered a pass.

nuisance immunity. A machine learning algorithm was implemented to study the prediction performance of using signals from either individual sensor or all sensors. The preliminary results highlighted the potential benefits of implementation of machine learning algorithms. Indeed, as the volume of data becomes larger and data complexity increases, advanced data processing, such as considering the rate of change of a sensor signal or ratios of signals from different sensors, may be beneficial to discriminate different cooking conditions.

Machine learning algorithms have the capability to transform a large set of complex data with multiple variables in meaningful ways, such that a hyperplane or a dynamic threshold can be obtained for classification problems. In fact, data-driven analytics have been used to resolve complex problems for a variety of applications. In structural engineering [14], a logistic regression model was used to provide failure detection of a shackle with a dual sensing system. For outage prediction of power grids [15,16], three-dimensional support vector machine (SVM) [17] were developed using limited data. Hand-crafted features were extracted to improve the performance of prediction. In the combustion community [18], a convolutional neural network was used to predict the likelihood of ignition for a hydrogen jet in air crossflow. However, no previous studies have been carried out to study the use of machine learning models that can classify pre-ignition conditions for different cooking scenarios. Using the experimental data collected in [13], this paper contributes the use of machine learning for development of robust and reliable early warning algorithms for sensor data. The developed algorithm can help to automatically cut cooktop power or gas flow to prevent cooktop ignition.

The rest of this paper is divided into four sections. Section 2 presents the experimental apparatus and procedure. Section 3 presents detailed descriptions associated with the proposed machine learning models. Section 4 discusses the results and key findings. Conclusions are provided in Section 5.

## 2. Experimental Apparatus and Procedure

Here, the focus is on electric coil element cooktop fires although some experiments were conducted using a gas cooktop. The experimental apparatus and procedure have been previously described in [12,13,19]. Some details are included here to provide a general description of the work.

### 2.1 General Setup

A series of 60 experiments were conducted in a mock kitchen, previously reported in [12,13]. A schematic of the experimental setup is shown in Figure 1. As seen in the figure, a cooktop/range is located between two gypsum-board cabinets. The dimensions of the cooktop/range are 68 cm in depth and 76 cm in width. The top surface of the cooktop/range was level with the standing cabinets. Two cooktops were considered: a household electric-coil cooktop with two heating element sizes and a household gas cooktop with three heating element sizes. For the electric-coil stove, both the big (20 cm) and the small (15 cm) heating elements were used. The heating power was measured as approximately 1.1 kW and 1.8 kW for the 15 cm and 20 cm electric-coils, respectively. For the gas cooktop, the estimated heating power was 4.0 kW for the large burner and 3.4 kW for the medium burner. The small gas burner was not used in the experiments.

An aluminum shroud was used in some of the experiments to reduce the influence of air circulation in the room.

## 2.2 Range Hood and Duct

Figure 1 shows the mock kitchen with a nominal 76 cm wide exhaust hood. The separation distance between the bottom surface of the range hood and the upper surface of the cooktop was 84 cm. The range hood was a 200-CFM (approximately 0.1 $m^3/s$) rated venting system to remove smoke, grease, odors, and moisture from the cooking space. The fan had variable flow control. The outlet of the range hood was connected to a nominal 15 cm diameter aluminum duct and the exhaust air was vented to the outside environment. The exhaust flow was characterized using a velocity probe at the center of the duct after the sensor array. The average flow speed and its standard deviation was 3.4 m/s ± 0.1 m/s over all the experiments. Using the electric coil cooktop, the duct temperature increased by an average of 9 °C during cooking, causing an estimated reduction in duct mass flow of 3 %. For the gas cooktop, the duct temperature increased by an average of 23 °C, which is estimated to reduce the duct mass flow by 7 %. The duct length between the range hood opening and the sensors was approximately 3 m.

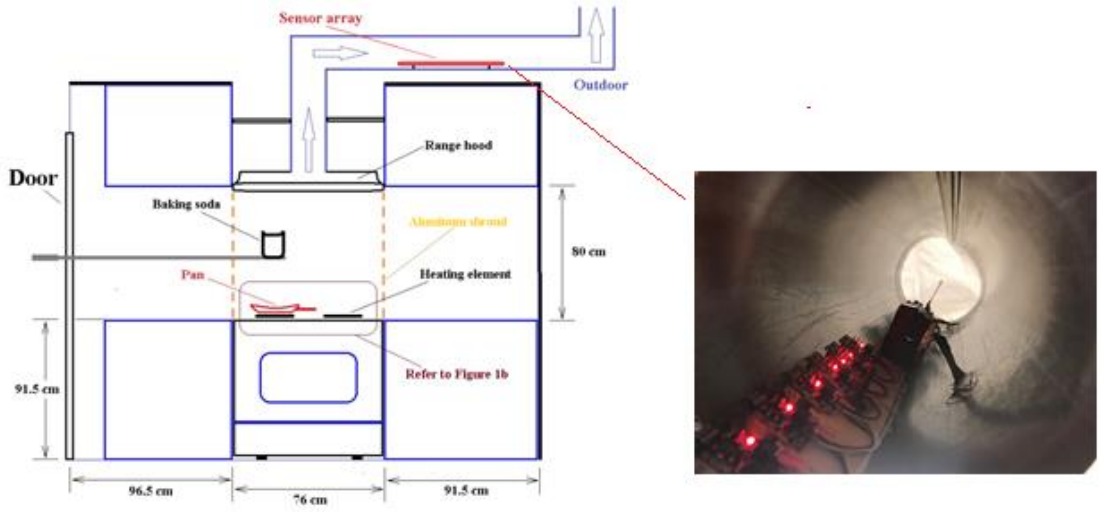


Figure 1. Schematic drawing of experimental setup (not to scale) and close-up view of the sensor array (in the duct).

## 2.3 Sensor Array

Figure 1 shows the sensor array secured inside the duct. There were 14 different sensors which are sensitive to smoke, alcohol, hydrocarbons, hydrogen, natural gas, carbon monoxide, volatile organic compounds (VOC), dust/aerosols, humidity, flow, indoor air quality (IAQ), temperature, and carbon dioxide. The dust sensor was modified from a commercial product to extend its range of sensitivity. Appendix A provides additional information for the sensor array.

## 2.4 Cooking Pans

A number of cooking pans were used in the experiments. The pans were either 20 cm or 25 cm diameter round pans. Four different types of pan materials were considered: cast iron, aluminum, stainless-steel, and a 5-layer aluminum/stainless-steel composite. Most of the experiments used the 20 cm cast iron pan, which is the cookware specified in the new UL 858 standard test [2]. It

should also be noted that Type-K thermocouples were spot-welded or peened onto the top surface of each pan to monitor its temperature. In general, there were two thermocouples used to measure the pan temperature: one at the center of the pan, and one closer to the edge. Thermocouples were used to monitor the stage of cooking. For the 20 cm cast iron pan on the small electric burner, the temperature towards the edge of the pan was about 23 °C higher than the center temperature. For experiments that only measured the temperature in the center of the pan, the temperature closer to the edge was estimated using a linear regression of the relationship between the two temperatures from experiments that both temperatures were measured [13].

### 2.5 Food

A representative range of foods were considered, including cooking oil, butter, chicken legs, salmon, hamburger, bacon, and french fries. As mentioned in [12,13], the cooking oils tested included canola oil, corn oil, olive oil, sunflower oil, and soy oil. The most common experiment used 50 mL of oil, but larger volumes of oil were also considered. A list of important test conditions for all experiments is summarized in Appendix B.

### 2.6 Test Procedure and Data Acquisition

For most experiments, both oils and food samples were prepared and placed on the pan before turning on the burner. The pan was centered on the specified burner. The gas or electric burner was generally set to its maximum power setting, and the output from the sensors was monitored. Data acquisition started at least 180 s before the heating element was turned on. Experiments were conducted until the food samples ignited or charred, or until normal cooking was complete. If ignition occurred, the fire was extinguished immediately by remotely applying baking soda. The range hood was kept turned on for the entire test period. Background signal values for each sensor, obtained before the burners were turned on, were subtracted from the raw signals. LabVIEW was utilized and an in-house program was coded to facilitate data acquisition. The sampling rate was set to 0.25 Hz. In total, data was obtained across over 12 800 time points.

## 3. Procedure for Machine Learning

Depending on the nature of the data (i.e., time series, images, text), the optimal machine learning architecture may be different. However, the overall workflow is relatively the same. After data collection, there are five primary steps: data profiling, preprocessing, feature selection, training and evaluation.

### 3.1 Data profiling

Figure 2 shows the data for 11 selected sensors together with the pan temperature for Exp. 8, which tested 50 mL of canola oil in a round 20 cm cast iron pan on a small electric cooktop burner set to maximum power at time = 0. When the pan temperature is below 200 ºC, there is nearly no change to any of the sensor signals. At approximately 230 ºC, most of the signals begin to rise increase rather monotonically, which was generally true for all the oil experiments. The red dashed line indicates the cooking condition, either normal or pre-ignition. The curve changes from 0 to 1 when the pan temperature exceeds 300 ºC at about 320 s. At 704 s, the pan temperature reached 429 ºC, and auto-ignition occurred; the test was immediately terminated.

Figure 3 shows 3 sets of curves for Exp 8 (solid line)[3], Exp 46 (circle symbols)[4], and Exp 57 (triangle symbols)[5]. Each set of curves contain the sensor signals for IAQ (black) and VOC (green), as well as the red line denoting the end of normal cooking and the beginning of the pre-ignition condition. Sensor data were selected based on the clear independence of the sensor signals from each other. For the two oil experiments (Exp 8 and Exp 57), the IAQ signals monotonically increased with time. However, the profile of the IAQ signal associated with Exp 46 was observably different; it first increased to a value of 0.3 x $10^4$, remained constant for more than 300 s, then increased to a peak value of 0.76 x $10^4$, reached a minimum value of 0.4 x $10^4$, before obtaining another peak value of 1.1 x $10^4$. The VOC sensor for Exp 46 also shows the same complex behavior. The physical mechanism causing such behavior is not known. However, this test was repeated and the same behavior was observed. Sensor data associated with all experiments were examined; Exp 16 was eliminated because the pan was not cleaned before the experiment such that a layer of degraded oil was on the bottom of the pan before the fresh oil was added. In the future, this type of experiment could be considered.

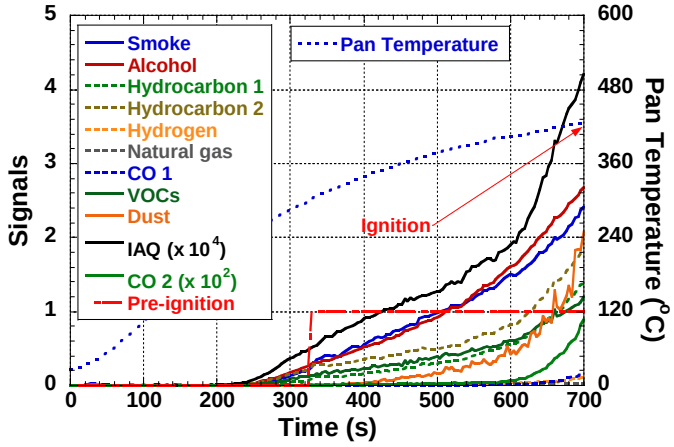


Figure 2. Signals for 11 selected sensors during Experiment 8.

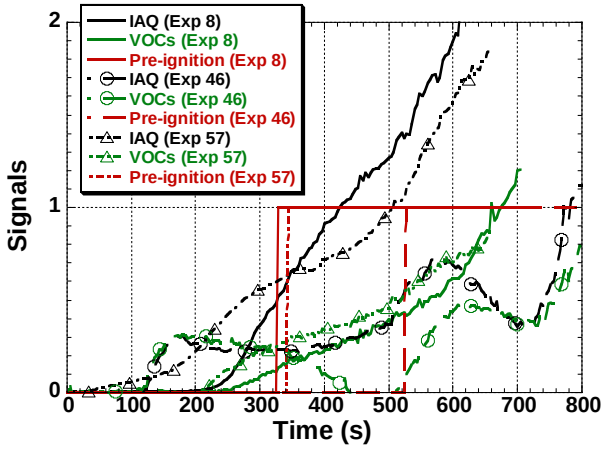


Figure 3. Comparison of IAQ (divided by $10^4$) and VOC signals for 3 experiments (8, 46, 57).

[3] Exp 8 is for 50 mL canola oil on a 20 cm cast iron pan heated by the small electric-coil burner.
[4] Exp 46 is for 110 g bacon on a 20 cm cast iron pan heated by the small electric-coil burner.
[5] Exp 57 is for 50 mL canola oil on a 20 cm cast iron pan heated by the big gas burner.

### 3.2 Preprocessing

As illustrated in Fig 2, the data range significantly differed between some of the sensor signals. For instance, in Exp 8 the data range of the smoke signal was from 0 to 2.5 V, while the IAQ signal range was more than 48 000. The difference in magnitude associated with the data is known to affect training efficiency, so a min-max normalization was applied to all signals to impose a range from 0 to 1.

In machine learning, a classifier is applied to a set of data instances that are well-annotated. The classifier learns the data distribution, or fits a hyperplane in multi-dimensional space, to separate data instances based on feature vectors and corresponding labels. Here, data instances are generated using a moving window. The advantage of this approach is to provide more information for each data instance, such as temporal information for the historical data.

The analysis applies a moving time window of size, $W$, as demonstrated in Figure 4. Each moving window represents one data instance. The measurement frequency of each signal was $f$ = 0.25 Hz (1 sample every 4 s) and there were $W$ x $f$ sample points for each signal in a moving window. Six signals are considered here, measuring alcohol, CO, dust, indoor air quality (IAQ), smoke, and VOC, leading to 6 time series with $W$ x $f$ sample points for each instance of processed data.

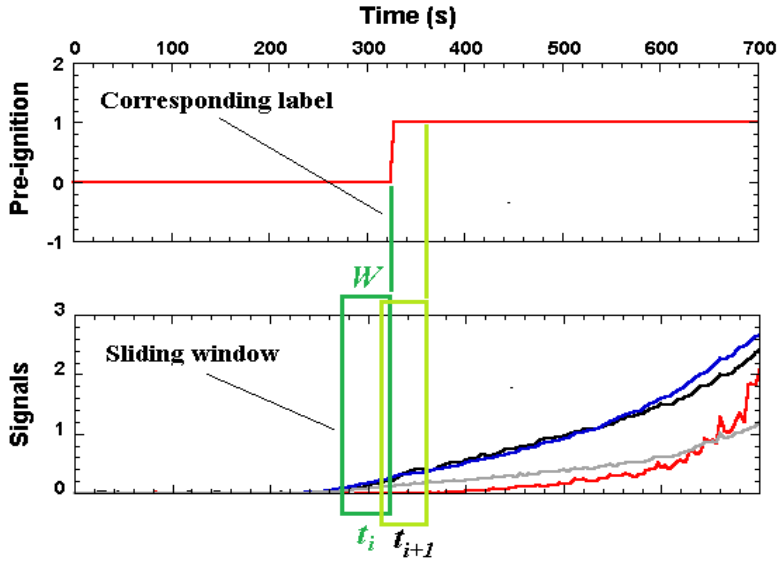


Figure 4. Schematic of moving windows with window size, $W$, and its corresponding label (the two sliding windows are not to scale; $t_i$ and $t_{i+1}$ are 4 s apart).

Table 1. Number of normal cooking and pre-ignition data instances for different groups of experiments when $W$ = 60 s.

| Group Label | Food type | Cooktop type | Normal cooking | Pre-ignition |
|---|---|---|---|---|
| OE (Oil, Electric) | Oil | Electric | 2486 | 2249 |
| OFE (Other Foods, Electric) | Other foods | Electric | 2702 | 606 |
| OG (Oil, Gas) | Oil | Gas | 675 | 1022 |
| All (OE+OFE+OG) | All | All | 5863 | 3877 |

In addition to feature representation, each instance also needs to be well annotated. As shown in Fig 4, each data instance was labeled "*Normal cooking*" or "*Pre-Ignition*". For oils, the data is defined as "*Normal Cooking*" if the pan temperature is less than 300 ºC. Reference [13] provides detailed descriptions for the determination of normal condition for other foods, such as salmon, bacon, chicken, hamburgers, and french fries. Table 1 illustrates data distributions for different groups of experiments with $W$ = 60 s. Depending on the size of time window ($W$), it should be noted that several instances (i.e. $W$ x $f$ – 1) will be lost.

### 3.3 Feature selections

After obtaining the processed data instances, features are extracted to build classifiers. Statistics, such as the mean, maximum, and standard deviation, are used to characterize a series of data or approximate the data distribution. These statistic-based representations may be useful to detect pre-ignition. For instance, pre-ignition is usually associated with high values of IAQ signal, so the maximum of the IAQ signal would be useful. We therefore propose a set of statistic-based features for unattended cooking detection.

Statistic-based features can represent the character of the data. However, they cannot capture the temporal or trend information. In order to extract this information, we also propose a set of trend-based features. Given the values of the signal within the data window, $S = [s_1, \dots, s_{n/2}, \dots, s_n]$, we extract trend-based features by computing: $s_n - s_1$, $s_{n/2} - s_1$, $s_n - s_{n/2}$, and max($S$) – min($S$). In addition to the raw signal, the first derivative is also calculated. We further extract the same set of features from the first derivative signal $S' = [s'_1, \dots, s'_{n/2}, \dots, s'_{n-1}]$, where $s'_i = s_{i+1} - s_i$. In total, 18 features for one signal can be extracted. As shown in Table 2, signals from 6 sensors, including alcohol, CO, dust, IAQ, smoke, and VOC are used. With these signals, a feature vector of 108 dimensions for each data instance is obtained. The feature vector is fed into a classifier to build the pre-ignition detection model.

Table 2. Signals and their features.

| **Sensors** | Alcohol | CO | Dust | IAQ | Smoke | VOC |
|---|---|---|---|---|---|---|
| **Signals** | Raw signal ($S$) and the first derivative ($S'$) | | | | | |
| **Trend-based features** | $s_n - s_1$, $s_{n/2} - s_1$, $s_n - s_{n/2}$, max($S$) – min($S$)<br>$s'_{n-1} - s'_1$, $s'_{(n-1)/2} - s'_1$, $s'_{n-1} - s'_{(n-1)/2}$, max($S'$) – min($S'$) | | | | | |
| **Statistical features** | Mean, maximum, minimum, median, standard deviation | | | | | |

### 3.4 Training and evaluation

The features introduced above are extracted for each instance, and then fed into a conventional machine learning algorithm to build the pre-ignition detection model. In this analysis, multiple machine learning algorithms are adopted for the detection model, including support vector machine (SVM), random forest (RF) [20], and decision tree (DT) [21]. These commonly used machine learning algorithms are reliable for many classification applications. Appendix C provides the basic concept and the model configuration for the three machine learning algorithms. Investigating and comparing the performance of these machine learning algorithms can help determine the most suitable machine learning model for ignition detection. In general, there is a tradeoff in real-time detection associated with the size of the moving window. Using a smaller moving window can increase the response time of the model, which is an important

factor in real-time detection. On the other hand, using a larger moving window is likely to achieve higher accuracy, as the model has more information. Therefore, the impacts of algorithm type as well as window size are investigated here. Three window sizes are considered: 60 s, 32 s, and 16 s based on the frequency of the input signal (0.25 Hz).

For evaluation purposes, a leave-one-experiment-out cross-validation approach is used. The dataset is divided into $N$ subsets, where $N$ is the total number of experiments. Each subset contains all the data instances from one particular experiment, then the classifier is trained with $N$ - 1 subsets and the classifier predictions are evaluated for the data instances in the remaining subset. This is repeated $N$ times until all the subsets are evaluated once. Final performance is taken as the overall average accuracy across all data instances in the $N$ evaluations.

## 4. Results and Discussion

### 4.1 Classification of unattended cooking for OE and OFE data

Data associated with all experiments[6] with oil on the electric cooktop (denoted as OE in Table 1) and other foods (OFE) on the electric cooktop were considered. Figure 5 shows an example of the prediction results of SVM with a moving window of 16 s for Exp 8 and Exp 46. The black curves are the classifier predictions. Blue curves are the converted values based on a discrimination threshold of 0.5. If the prediction value is less than 0.5, the prediction is classified as normal cooking. If the prediction is larger than 0.5, the prediction is classified as pre-ignition. As compared to the data label (red curves), the SVM tends to predict pre-ignition well before the ignition. In order to evaluate the performance over all experiments, the precision, recall, and F1-score measures are reported. Table 3 shows the prediction performance for the three moving window sizes. Here, precision is defined as the ratio of the number of true positives over the sum of true and false positives; recall is defined as the ratio of true positives over sum of true positives and false negatives. The F1 score is the weighted average of precision and recall.

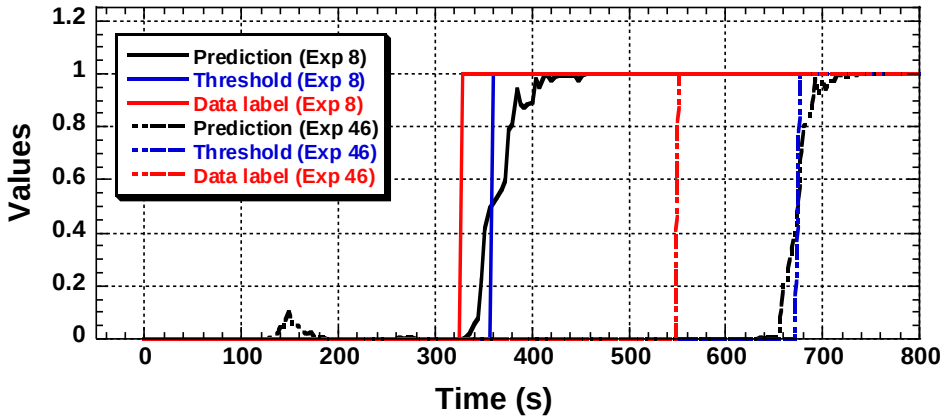


Figure 5. Performance comparison of SVM with $W$ of 16 s for Exp 8 and Exp 46 considering both OE and OFE data.

[6] Exp 16, 39, 48, 49, 50, and 60 are excluded. Exp 39, 48, 50 and 60 are dual-pan experiments. Since single pan experiments are of interest, the dual-pan experiments will be considered in future study.

The Correct Classified Rates (CCR) for the three machine learning models with three moving window sizes are presented in Fig 6. CCR is defined as the ratio of the correct classified instances to the total instances in a dataset; it is an indicator of overall classification performance. The results in Fig. 6 suggest two general conclusions. First, the larger the window size, the better the observed performance. Second, SVM seems to have slightly higher CCRs compared to RF and DT. For SVM, prediction accuracies are 93.8 %, 92.8 %, and 91.2 % for $W$ = 60 s, 32 s, and 16 s, respectively. This statistic demonstrates that with approximately 4 times the detection frequency, there was only a 2.5 % tradeoff on prediction accuracy.

Table 3. Precision, recall, and F1-score for SVM with three moving window sizes considering both OE and OFE data.

| Window size | Class | Precision | Recall | F1-score |
|---|---|---|---|---|
| 60 s | Normal | 96.3% | 94.1% | 95.2% |
| | Unattended | 89.7% | 93.4% | 91.5% |
| 32 s | Normal | 94.9% | 93.8% | 94.3% |
| | Unattended | 89.3% | 91.1% | 90.1% |
| 16 s | Normal | 93.6% | 92.4% | 93.0% |
| | Unattended | 87.2% | 89.1% | 88.1% |

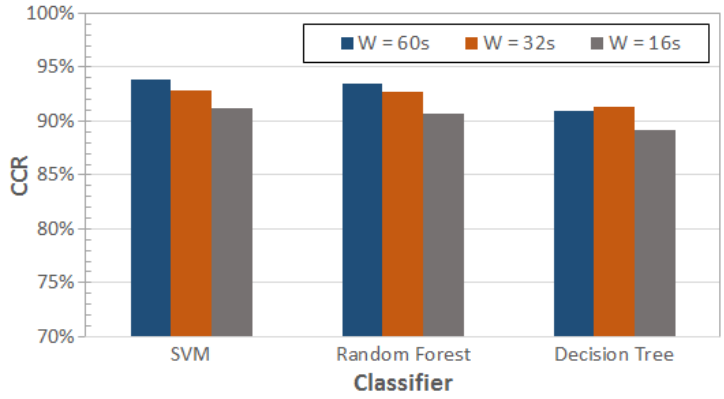


Figure 6. Overall performance classifying normal cooking and pre-ignition for three machine learning models with different moving window sizes considering both OE and OFE data.

## 4.2 Classification of pre-ignition using an object-specified approach

Sensors in the oil experiments, regardless of oil volume, oil type, and heating conditions, presented monotonic behavior. This trend does not necessarily exist for the cooking experiments with other foods due to a variety of factors including possibly the burner settings used, the water content of the foods, and the shape and deformation of the foods during cooking. If a machine learning model uses data that have similar behaviors, the prediction performance should increase. Therefore, an object-specified approach was also followed, training and evaluating the machine learning models either with only the OE data or only the OFE data.

Figure 7 shows the updated CCRs using the object-specified approach on SVM. For OE data alone, the prediction performance for $W$ = 60 s is increased over the combined OE and OFE data to 96.9 %. In general, there is an average 1.9 % improvement in the prediction performance over the combined OE and OFE data for all three moving window sizes. For OFE data alone, the

prediction performance for $W$ = 16 s increases by 5.1 % over the combined OE and OFE data. The improved performance for OFE data alone with $W$ = 60 s and $W$ = 32 s is 2 % and 2.8 %, respectively. Table 4 shows the detailed breakdown of the two data sets using statistical measures, showing the enhanced prediction accuracy.

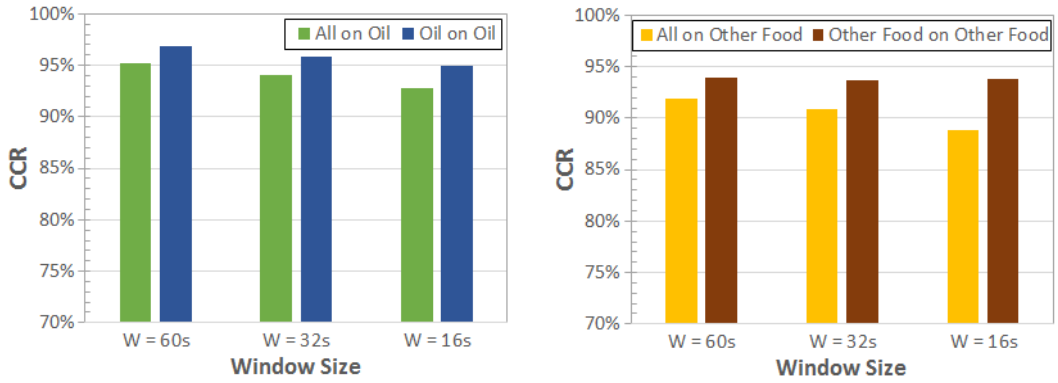


Figure 7. Performance of SVM predictions using both OE and OFE data for training compared to the object-specified approach, where only OE or OFE data is used for training.

Table 4. Precision, recall, and F1-score for SVM with three moving window sizes using the object-specified approach.

| Dataset | Class | Precision | Recall | F1-score |
|---|---|---|---|---|
| Oil (OE) | Normal | 98.4% | 95.7% | 97.0% |
| | Unattended | 95.3% | 98.2% | 96.8% |
| Other Foods (OFE) | Normal | 96.8% | 95.8% | 96.2% |
| | Unattended | 82.0% | 85.6% | 83.8% |

### 4.3. Towards Two-Step Pre-Ignition Detection

Based on the previous section, the object-specified machine learning models built to classify the cooking conditions (normal or pre-ignition) for a specific type of cooking (oil heated on an electric cooktop versus other foods on an electric cooktop) is shown to outperform the more generic machine learning model. This performance enhancement does not require additional data. Instead, to use the object-specified machine learning models, a classifier that discriminates between the oil cooking scenarios and other cooking scenarios is needed. The gas cooktop experiments were not included in the previous analyses, so cooktop type could also be important in determination an optimized model. Nevertheless, the feasibility of use of a two-step architecture for detection of pre-ignition is investigated.

Next, machine learning is used to detect the type of cooktop being used. The cooking oil results from different cooktop types in the dataset are used. The data from heating oil on an electric cooktop (OE) are given the label "*Electric*", and the data from heating oil on a gas cooktop (OG) are given the label "*Gas*". The same features as presented in Section 3.3 are used to build the cooktop type identification models and the same evaluation approach is adopted. As shown in Fig. 8, the attempt leads to very promising performance of cooktop identification. Using SVM as the classifier with $W$ = 60 s, an accuracy of better than 98 % is observed. For a smaller $W$, which enables a faster time response, an accuracy of 98 % ($W = 32\ s$) and 97.3 % ($W = 16\ s$) is

achieved. As shown in Table 5, the models achieve high F1-scores for both cooktop types, indicating that the model does not achieve high CCR by simply selection of the majority side. These results suggest that the proposed method can precisely differentiate an electric cooktop from a gas cooktop, providing verification of the machine learning methods developed here. The results also demonstrate that it may be possible to build a two-step pre-ignition detection model, which first classifies the cooking scenario to recommend a specific model to better predict pre-ignition conditions for a particular type of cooktop.

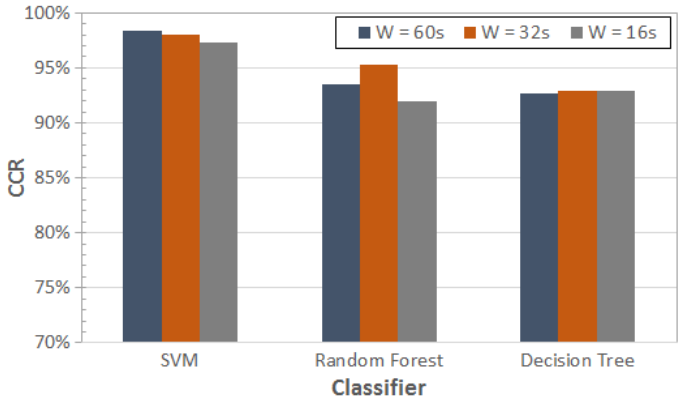


Figure 8. Overall performance on cooktop type classification for the three machine learning models with different *W* using OE and OG data sets.

Table 5. Precision, recall, and F1-score for SVM with three different *W* for cooktop type classification.

| Window size | Class | Precision | Recall | F1-score |
|---|---|---|---|---|
| 60 s | Electric | 99.5% | 98.4% | 98.9% |
| | Gas | 95.5% | 98.5% | 96.9% |
| 32 s | Electric | 98.9% | 98.4% | 98.7% |
| | Gas | 95.4% | 96.7% | 96.0% |
| 16 s | Electric | 98.1% | 98.2% | 98.2% |
| | Gas | 94.7% | 94.5% | 94.6% |

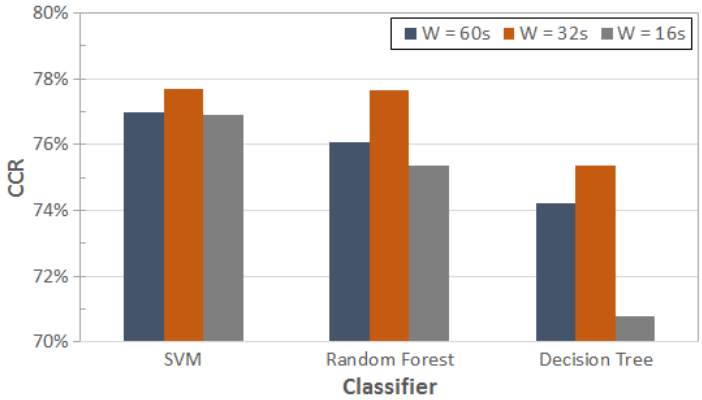


Figure 9. Overall performance on food type classification for the 3 machine learning models with different moving window size on OE and OFE data.

Next, the possibility of using the classifier to identify the heating of oil versus cooking scenarios involving foods is investigated. Both the OE and OFE data sets using the electric cooktop are utilized. The data with oil (OE) is labeled "*Oil*" and the data with other foods (OFE) is labeled "*Others*". The same model features and evaluation approach presented in Section 3.3 to build the oil versus other scenario detection models are adopted here. Table 6 provides the detailed statistical performance for the food type predictions. The numerical results indicate that the models cannot precisely differentiate cooking oil from scenarios involving cooking other foods. A possible reason is that there is insufficient data. The models to detect cooktop type achieved promising performance despite fewer data sets using the gas cooktop because the sensor signals from heating oil with a gas cooktop does not vary as much across different experiments as the varied data sets in the OFE data group. The types of other foods and procedures of cooking other foods are much more diverse than just heating oil on the highest setting, leading to diverse sensor signal patterns that make it difficult for the classifier to learn patterns.

Table 6. Precision, recall, and F1-score for SVM with three moving window sizes on classifying heating oil from other cooking scenarios on electric cooktops.

| Window size | Class | Precision | Recall | F1-score |
|---|---|---|---|---|
| 60 s | Oil | 74.9% | 92.6% | 82.8% |
| | Others | 82.9% | 53.4% | 65.0% |
| 32 s | Oil | 75.0% | 94.5% | 83.6% |
| | Others | 86.2% | 51.9% | 64.8% |
| 16 s | Oil | 74.2% | 94.6% | 83.2% |
| | Others | 85.7% | 49.6% | 62.8% |

## 5. Conclusions

The feasibility of building machine learning models to perform real-time cooktop pre-ignition detection is investigated. Machine learning algorithms have the capability to consider multiple sensor signals. Taking advantage of that capability, statistic-based and trend-based features are extracted from the time series signal of six sensors: alcohol, CO, dust, IAQ, smoke, and VOC, to build pre-ignition detection models. The proposed approach achieves encouraging performance, even when using data from diverse cooking scenarios on electric cooktops (OE and OFE data sets) for training with 93.8 % of data instances predicted correctly (using SVM and $W$ = 60 s).

Models trained and tested only on data for a specified cooking condition (separating OE and OFE data sets) outperform models trained on the combined set of all electric cooktop data. For instance, the overall accuracy is 96.9 % for the model trained and tested on only the OE data set (using SVM and $W$ = 60 s). If the cooking scenario of the target data can be identified, the detection performance of pre-ignition can be improved. This suggests the potential of a two-step approach to obtain a more robust cooking pre-ignition detection model.

Results from calculations to identify cooking scenarios using a multi-step detection approach shows it is possible to precisely differentiate heating oil on electric cooktop from a gas cooktop. However, the method was not as effective in identifying a scenario of heating oil versus cooking other foods on an electric cooktop. In the future, experiments on a wider variety of food types will be considered to test the range of possible improvement of model performance.

## Acknowledgement

The authors are very grateful to Dr. Michael Huang for helpful discussions and suggestions.

## Supplementary material

Sensor data associated with this article and that of obtained from [12,13] can be found at: https://doi.org/10.18434/M32171.

## References

[1] Ahrens, M., 2009. *Home fires involving cooking equipment*. Quincy: National Fire Protection Association.

[2] Underwriter's Laboratory, 2014 and 2018. Standard for Household Electric Ranges (UL 858). Northbrook IL.

[3] Hamins, A., Kim, S.C. and Madrzykowski, D., 2018. Characterization of stovetop cooking oil fires. *J Fire Sciences*, *36*(3), pp.224-239.

[4] Hamins, A., Kim, S.C. and Bundy, M., 2018. *Investigation of Residential Cooktop Ignition Prevention Technologies*. US Department of Commerce, National Institute of Standards and Technology.

[5] Gottuk, D.T., Wright, M.T., Wong, J.T., Pham, H.V. and Rose-Pehrson, S.L., 2002. *Prototype Early Warning Fire Detection System: Test Series 4 Results* (No. NRL/MR/6180--02-8602). NAVAL RESEARCH LAB WASHINGTON DC.

[6] Cestari, L.A., Worrell, C. and Milke, J.A., 2005. Advanced fire detection algorithms using data from the home smoke detector project. *Fire Safety Journal*, *40*(1), pp.1-28.

[7] Jain, A., Nyati, P., Nuwal, N., Ansari, A., Ghoroi, C.H.I.N.M.A.Y. and Ghandi, P., 2014. Pre-Detection of Kitchen Fires due to Auto-Ignition of Cooking Oil and LPG Leakage in Indian Kitchens. *Fire Safety Science*, *11*, pp.1285-1297.

[8] Johnsson, E. and Zarzecki, M., 2017. Using Smoke Obscuration to Warn of Pre-Ignition Conditions of Unattended Cooking Fires. In *16th International Conference on Automatic Fire Detection (AUBE'17) & Suppression, Detection and Signaling Research and Applications Conference (SUPDET 2017)*.

[9] Gaur, A., Singh, A., Kumar, A., Kulkarni, K.S., Lala, S., Kapoor, K., Srivastava, V., Kumar, A. and Mukhopadhyay, S.C., 2019. Fire Sensing Technologies: A Review. *IEEE Sensors Journal*, 19(9), pp.3191-3202.

[10] Fonollosa, J., Solórzano, A. and Marco, S., 2018. Chemical sensor systems and associated algorithms for fire detection: A review. *Sensors*, 18(2), p.553.

[11] Johnsson, E.L., 1998. Study of technology for detecting pre-ignition conditions of cooking-related fires associated with electric and gas ranges and cooktops, final report, NISTIR 5950, National Institute of Standards and Technology, Gaithersburg, Maryland.

[12] Mensch, A., Hamins, A. and Markell, K., 2018, September. Development of a Detection Algorithm for Kitchen Cooktop Ignition Prevention. In *Suppression, Detection and Signaling Research and Applications Conference Proceedings (SUPDET 2018)*.

[13] Mensch, A., Hamins, A., Lu, J., Kupferschmid, M., Tam, W.C. and You, C., 2019, September. Evaluating Sensor Algorithms to Prevent Kitchen Cooktop Ignition and Ignore Normal Cooking. In *Suppression, Detection and Signaling Research and Applications Conference Proceedings (SUPDET 2019)*.

[14] Jang, D.W., Lee, S., Park, J.W. and Baek, D.C., 2018. Failure detection technique under random fatigue loading by machine learning and dual sensing on symmetric structure. *International Journal of Fatigue*, 114, pp.57-64.

[15] Eskandarpour, R., Khodaei, A. and Arab, A., 2017, September. Improving power grid resilience through predictive outage estimation. In *2017 North American Power Symposium (NAPS)* (pp. 1-5). IEEE.

[16] Bhattacharya, B. and Sinha, A., 2017, November. Intelligent fault analysis in electrical power grids. In *2017 IEEE 29th International Conference on Tools with Artificial Intelligence (ICTAI)* (pp. 985-990). IEEE.

[17] Hearst, M.A., Dumais, S.T., Osuna, E., Platt, J. and Scholkopf, B., 1998. Support vector machines. *IEEE Intelligent Systems and their applications*, 13(4), pp.18-28.

[18] Popov, P.P., Buchta, D.A., Anderson, M.J., Massa, L., Capecelatro, J., Bodony, D.J. and Freund, J.B., 2019. Machine learning-assisted early ignition prediction in a complex flow. *Combustion and Flame*, 206, pp.451-466.

[19] Mensch, A., Hamins, A., Tam, W.C., Lu, J., Markell, K., You, C., and Kupferschmid, M., Sensors and Machine Learning Models to Prevent Cooktop Ignition and Ignore Normal Cooking. *Fire Technology (Submitted).*

[20] Breiman, L., 2001. Random forests. Machine learning, 45(1), pp.5-32.

[21] Kwok, S.W. and Carter, C., 1990. Multiple decision trees. In *Machine Intelligence and Pattern Recognition* (Vol. 9, pp. 327-335). North-Holland.

[22] Mishra, M., & Rout, P. K., 2017. Detection and classification of micro-grid faults based on HHT and machine learning techniques. *IET Generation, Transmission & Distribution*, *12*(2), 388-397.

[23] Kazem, H. A., Yousif, J. H., & Chaichan, M. T., 2016. Modeling of daily solar energy system prediction using support vector machine for Oman. *International Journal of Applied Engineering Research*, *11*(20), 10166-10172.

[24] Moutis, P., Skarvelis-Kazakos, S., & Brucoli, M., 2016. Decision tree aided planning and energy balancing of planned community microgrids. *Applied Energy*, *161*, 197-205.

[25] Jiang, H., Li, Y., Zhang, Y., Zhang, J. J., Gao, D. W., Muljadi, E., & Gu, Y., 2017. Big data-based approach to detect, locate, and enhance the stability of an unplanned microgrid islanding. *Journal of Energy Engineering*, *143*(5), 04017045.

[26] Vapnik, V., 1998. The support vector method of function estimation. In *Nonlinear Modeling* (pp. 55-85). Springer, Boston, MA.

[27] Breiman, L., 2017. *Classification and regression trees*. Routledge.

[28] Breiman, L., 2001. Random forests. *Machine learning*, *45*(1), pp.5-32.

[29] Oliphant, T.E., 2007. Python for scientific computing. *Computing in Science & Engineering*, *9*(3), pp.10-20.

[30] Staelin, C., 2003. Parameter selection for support vector machines. *Hewlett-Packard Company, Tech. Rep. HPL-2002-354R1*, *1*.

[31] Pedregosa, F., Varoquaux, G., Gramfort, A., Michel, V., Thirion, B., Grisel, O., Blondel, M., Prettenhofer, P., Weiss, R., Dubourg, V. and Vanderplas, J., 2011. Scikit-learn: Machine learning in Python. *Journal of machine learning research*, *12*(Oct), pp.2825-2830.

## Appendix A. Additional Information for Sensor Array.

14 different sensor responses were selected for testing. The sensors were based on various operating mechanisms, including electrochemical, MOS-type, light scattering, and non-dispersive infrared absorption. Sensors were selected to measure $CO_2$, CO, hydrocarbons, alcohols, $H_2$, natural gas, volatile organic compounds (VOCs), smoke, air quality, and aerosols/dust. Humidity and temperature were also measured. Table A1 provides the sensor names, their sensitivity, operating principle, measurement range, and units.

Table A1. Summary of sensor information.

| | Sensor Name | Sensitivity | Operating Principle | Measurement Range | Units |
|---|---|---|---|---|---|
| **1** | Smoke | combustible gas, smoke | electrochemical | 300 -10,000 | ppm |
| **2** | Alcohol | alcohol | electrochemical | 0.04 - 4 | mg/L |
| **3** | Hydrocarbon 1 | methane, propane, butane | electrochemical | 300 -10,000 | ppm |
| **4** | Hydrocarbon 2 | liquified petroleum, butane, propane, LPG | electrochemical | 300 - 10,000 | ppm |
| **5** | Hydrogen | $H_2$ | electrochemical | 100 - 1,000 | ppm |
| **6** | Natural Gas | methane | electrochemical | < 10,000 | ppm |
| **7** | CO 1 | CO | electrochemical | 0 - 10,000 | ppm |
| **8** | VOCs | air contaminants, VOCs, odorous gases | metal oxide sensor | not specified | ppm |
| **9** | Dust | aerosol | optical | 0.1 - 0.5 | $mg/m^3$ |
| **10** | Humidity | $H_2O$ | electrochemical | 2000 | ppm |
| **11** | $CO_2$ 1 | $CO_2$ | electrochemical | 2000 | ppm |
| **12** | IAQ | cooking odors, pollutants, smoke | electrochemical | not specified | ppm |
| **13** | $CO_2$ 2 | $CO_2$ | electrochemical | 5000 | ppm |
| **14** | CO 2 | CO | electrochemical | 5000 | ppm |

491

## Appendix B. Summary of important experimental information.

| EXP | Ignition | Pan Type and Size (cm) | Food Type and Amount | Burner Type and Size | Hood Flow | Foil Surround |
|---|---|---|---|---|---|---|
| 1 | Yes | Cast Iron, 20 | Canola Oil, 50mL | Electric, Small | High | No |
| 2 | Yes | Cast Iron, 20 | Canola Oil, 50mL | Electric, Small | High | No |
| 3 | Yes | Cast Iron, 20 | Canola Oil, 50mL | Electric, Small | High | No |
| 4 | Yes | Cast Iron, 20 | Canola Oil, 50mL | Electric, Small | High | No |
| 5 | Yes | Cast Iron, 20 | Canola Oil, 50mL | Electric, Small | High | No |
| 6 | Yes | Cast Iron, 20 | Canola Oil, 50mL | Electric, Small | High | No |
| 7 | Yes | Cast Iron, 20 | Canola Oil, 50mL | Electric, Small | High | No |
| 8 | Yes | Cast Iron, 20 | Canola Oil, 50mL | Electric, Small | High | No |
| 9 | Yes | Cast Iron, 20 | Canola Oil, 100mL | Electric, Small | High | No |
| 10 | Yes | Aluminum, 20 | Canola Oil, 50mL | Electric, Small | High | Yes |
| 11 | Yes | Multi-layered, 20 | Canola Oil, 50mL | Electric, Small | High | Yes |
| 12 | Yes | Stainless Steel, 20 | Canola Oil, 50mL | Electric, Small | High | Yes |
| 13 | Yes | Cast Iron, 20 | Canola Oil, 200mL | Electric, Small | High | Yes |
| 14 | Yes | Cast Iron, 20 | Canola Oil, 50mL | Electric, Big | High | Yes |
| 15 | Yes | Cast Iron, 25 | Canola Oil, 100mL | Electric, Big | High | Yes |
| 16 | No | Aluminum, 20 | Corn Oil, 50mL | Electric, Small | High | No |
| 17 | Yes | Aluminum, 20 | Corn Oil, 50mL | Electric, Small | High | No |
| 18 | Yes | Cast Iron, 20 | Corn Oil, 50mL | Electric, Small | High | No |
| 19 | Yes | Cast Iron, 25 | Corn Oil, 100mL | Electric, Big | High | Yes |
| 20 | Yes | Cast Iron, 20 | Corn Oil, 50mL | Electric, Small | High | Yes |
| 21 | Yes | Cast Iron, 20 | Soy Oil, 50mL | Electric, Small | High | Yes |
| 22 | Yes | Cast Iron, 25 | Soy Oil, 100mL | Electric, Big | High | Yes |
| 23 | Yes | Cast Iron, 20 | Olive Oil, 50mL | Electric, Small | High | Yes |
| 24 | Yes | Cast Iron, 25 | Olive Oil, 100mL | Electric, Big | High | Yes |
| 25 | Yes | Cast Iron, 25 | Sunflower Oil, 100mL | Electric, Big | High | Yes |
| 26 | Yes | Cast Iron, 20 | Sunflower Oil, 50mL | Electric, Small | High | Yes |
| 27 | Yes | Cast Iron, 20 | Butter, 45.68g | Electric, Small | High | Yes |
| 28 | No | Broiler Pan | Hamburger, 1.14kg | Oven | High | NA |
| 30 | No | Cast Iron, 25 | Hamburger, 1.14kg | Electric, Big | High | Yes |
| 31 | Yes | Cast Iron, 20 | Salmon, 18oz & Butter 42.5g | Electric, Small | High | Yes |
| 32 | No | Cast Iron, 25 | Salmon, 2.8oz & Butter 85.1g | Electric, Big | High | Yes |
| 33 | No | Cast Iron, 20 | Water, 50mL | Electric, Small | High | Yes |
| 34 | No | NA | NA | Electric, Big | High | NA |
| 35 | Yes | Cast Iron, 20 | Canola Oil, 50mL | Electric, Small | High | No |
| 36 | Yes | Cast Iron, 20 | Canola Oil, 50mL | Electric, Small | Medium | No |
| 37 | No | Cast Iron, 20 | Canola Oil, 50mL | Electric, Small | Medium | No |
| 38 | No | Aluminum, 20 | Canola Oil, 50mL | Electric, Small | Medium | No |
| 39 | No | Cast Iron, 20 & Aluminum, 20 | Canola Oil, 50mL & Canola Oil, 50mL | Electric, Big & Electric, Small | Medium | No |
| 40 | No | Cast Iron, 20 | Canola Oil, 50mL | Electric, Small | Off | No |
| 41 | No | Broiler Pan | Hamburger, 1.14kg | Oven | High | NA |

| EXP | Ignition | Pan Type and Size (cm) | Food Type and Amount | Burner Type and Size | Hood Flow | Foil Surround |
|---|---|---|---|---|---|---|
| 42 | No | Cast Iron, 20 | Salmon, 18oz & Butter 42.4g | Electric, Small | High | No |
| 43 | No | Cast Iron, 20 | Chicken legs, 2 pieces & Canola Oil, 200mL | Electric, Small | High | No |
| 44 | Yes | Cast Iron, 25 | French fries, 223.3g & Canola Oil, 500mL | Electric, Big | High | No |
| 45 | No | Cast Iron, 25 | Bacon, 228g | Electric, Big | Medium | No |
| 46 | Yes | Cast Iron, 20 | Bacon, 110g | Electric, Small | Medium | No |
| 47 | No | Cast Iron, 25 | Hamburger, 1.14kg | Electric, Big | Medium | No |
| 48 | Yes | Cast Iron, 20 & Cast Iron, 25 | Canola Oil, 50mL & Canola Oil, 100mL | Electric, Big & Electric, Small | High | No |
| 49 | Yes | Cast Iron, 20 & Cast Iron, 25 | Canola Oil, 50mL & Canola Oil, 100mL | Electric, Big & Electric, Small | High | No |
| 50 | Yes | Cast Iron, 20 & Cast Iron, 25 | Canola Oil, 50mL & Canola Oil, 100mL | Electric, Big & Electric, Small | High | No |
| 51 | Yes | Cast Iron, 20 | Canola Oil, 50mL | Electric, Small | Low | No |
| 52 | No | NA | NA | Gas, Big | Medium | No |
| 53 | No | Cast Iron, 20 | Canola Oil, 50mL | Gas, Medium | Medium | No |
| 54 | Yes | Cast Iron, 25 | Canola Oil, 100mL | Gas, Big | Medium | No |
| 55 | No | Cast Iron, 25 | NA | Gas, Big | Medium | No |
| 56 | Yes | Cast Iron, 25 | Canola Oil, 100mL | Gas, Big | Medium | No |
| 57 | Yes | Cast Iron, 20 | Canola Oil, 50mL | Gas, Big | Medium | No |
| 58 | Yes | Cast Iron, 25 | Canola Oil, 100mL | Gas, Big | Medium | No |
| 59 | No | NA | NA | Gas, Big | Medium | No |
| 60 | No | Cast Iron, 20 & Cast Iron, 25 | Canola Oil, 50mL & Canola Oil, 100mL | Gas, Big & Gas, Medium | Medium | No |

492

493 It should be noted that all sensor data listed in this appendix can be found at
494 https://doi.org/10.18434/M32171.

## Appendix C. Basic Concept for Support Vector Machine, Decision Tree, and Random Forest.

Machine learning (ML) algorithms have been widely used for multi-class classification problems in various fields. Based on recent literature [22-25], it has been demonstrated that support vector machine (SVM), decision tree (DT), and random forest (RT) have the capabilities to handle complex time series data with multi-dimensional feature vectors. Guidelines are lacking for the use of ML algorithms in classification problems involving time series data in fire research, and the performance for these three ML algorithms is unknown. Therefore, SVM, DT, and RF will be used for the development of classification models for prediction of fire hazards. Comparing the results obtained from the different models can serve as a sanity check for the performance of each model. In the next subsection, the basic concepts for SVM, DT, and RT will be presented. Readers can refer to the following references [26-28] for detailed descriptions of the mathematical formulation for each algorithm.

Support Vector Machine (SVM) [26]

SVM is a classifier that finds a decision boundary, known as a hyperplane, to separate instances into two classes. The algorithm maximizes the constrained margin such that the distance between the instances in different classes is optimized to achieve the greatest model generalizability. For example, given a training dataset $T = \{(X_1, y_1), (X_2, y_2), \dots, (X_n, y_n)\}$ , which can be linearly separated, the hyperplane denoted as $p$ can be written as:

$$w \bullet X + b = 0 \tag{C1}$$

where $X_n$ is the sample of $n^{th}$ instance, and $y_n$ is the class label. $w$ is the weight of the hyperplane, and $b$ is the bias of the hyperplane. Based on the definition provided in [26], the distance between the instances for different classes is:

$$d = \min_{i=1,2,\dots,n} y_i\left(\frac{w}{\|w\|} \cdot X_i + \frac{b}{\|w\|}\right) \tag{C2}$$

where $\|w\|$ is norm of $w$. For SVM, the distance is known as margin. Therefore, SVM determines the hyperplane with the largest margin by solving the optimization problem:

$$\arg\max_{w,b} \left(\min_{i=1,2,\dots,n} y_i\left(\frac{w}{\|w\|} \cdot X_i + \frac{b}{\|w\|}\right)\right) \tag{C3}$$

For real-life applications, fire data are often more complex and not linearly separable. In order to overcome this numerical difficulty, there are two treatments. The first treatment is called the "kernel trick" [26], which commonly involves four nonlinear kernel functions: 1) polynomial kernel, 2) Gaussian kernel, 3) radial basis function, and 4) sigmoid kernel. The use of a kernel function allows the transformation of data into a higher dimensional space such that a hyperplane exists separating the instances $X_n$ for different classes. The second treatment is introducing a regularization or slack variable. With the implementation of the regularization variable, a small proportion of the data are ignored, and misclassification is allowed. Although there is trade-off

for use of the regularization variable treatment, it generally helps to avoid over-fitting and to provide a more generalized model.

Decision Tree (DT) [27]

DT builds classification models in the form of a tree structure. A typical DT is composed of a root node, internal nodes, edges, and leaves. The root node represents the entire population. Internal nodes represent partitioning or splitting conditions, which correspond to a feature vector. Edges can be a specific value or range of values for the splitting condition of the feature. The leaves represent the terminal nodes of a tree with class labels. The hierarchical nature of the algorithm provides detailed information of how a decision is being made. As compared to SVM, DT is more transparent, and the results are easier to interpret.

Given the aforementioned training dataset $T = \{(X_1, y_1), (X_2, y_2), \dots, (X_n, y_n)\}$, the formulation of a DT involves selecting optimal splitting features. The process starts by splitting the dependent feature, or root node, into binary pieces, where the child nodes have less entropy than the parent node. If the sample is completely homogeneous the entropy is zero, and if the sample is equally divided the entropy is one. Mathematically, entropy is defined as:

$$Entropy = -\sum_{i=i}^{k} P_k log P_k \tag{C4}$$

where $P_k$ is possibility of the instance belonging to class $k$. In general, DT searches through all candidate splits to find the optimal split that minimizes the resulting entropy of a tree. One effective split strategy is to always select the feature with largest information gain, $IG$:

$$IG(D_p, f) = Entropy(D_p) - \sum_{i}^{all\ child\ node} \frac{N_i}{N} Entropy(D_i) \tag{C5}$$

where $D_p$ is the dataset of the parent node with $N$ number of samples, $f$ is the feature, and $D_i$ is the dataset of the $i^{th}$ child node with $N_i$ number of instances. This splitting process is continued until all the instances at current level are labeled to the appropriate classes.

Random Forest (RF) [28]

RF is an ensemble learning method for classification. It builds $H$ number of classification trees and provides the prediction of the class of an object based on the averaged results obtained from each of the trees. Mathematically, after $H$ trees are grown, the RF classification predictor is given as:

$$f(x) = \frac{1}{H} \sum_{i=1}^{H} K(i, x) \tag{C6}$$

where $x$ is the input feature.

In general, significant effort is usually needed to tune the model to maximize performance. This process can be accomplished by selecting appropriate hyperparameters, which can be thought of as the "dials" or "knobs" of a machine learning model. There are several automated tuning methods, such as grid search, random search, and Bayesian optimization. In this study, the most basic tuning method, grid search [29], is used. With this technique, we simply build a model for each possible combination of all the hyperparameter values provided, evaluate each model, and select the architecture which produces the best results.

Summary

Table C1 provides the summary of model configurations for the three ML algorithms. For SVM, the radial basis functions (RBF) kernel function is used. The selection of the kernel function depends on both the number of input features and the size of the dataset. In this study, there are up to 12 features and roughly 10000 instances (refer to Table 1). Since the number of samples from the dataset is much larger than the number of input features, it is suggested that RBF will have better performance [30]. With the use of the RBF kernel, the two parameters, $C$ and $\gamma$, must be considered. The parameter $C$ is the regularization parameter or slack variable, and it controls the trade-off between misclassification of training examples and simplicity of the decision surface. In general, a low $C$ makes the decision surface smooth, while a high $C$ aims to classify all training examples correctly [31]. The parameter $\gamma$ defines how much influence a single training example has on other examples. The larger $\gamma$ is, the less influence a single simple will have. Grid search [29] is used to determine the optimal values for the two parameters.

Table C1: Summary of model configurations for SVM, DT, and RF.

| **SVM** | | | | **DT** | **RF** | | | |
|---|---|---|---|---|---|---|---|---|
| | **Optimal** | **Range** | **Interval** | | | **Optimal** | **Range** | **Interval** |
| ***C*** | 100 | 0 - 300 | 10 | NA | **Estimator** | 10 | 5 - 100 | 5 |
| **Gamma ($\gamma$)** | 10 | 0 - 50 | 1 | | | | | |

The model configurations for DT and RF are simpler. For DT, the entropy method is used to measure the quality of a split, but no parameters were needed to be adjusted. For RF, the setting remains similar except that the optimal number of trees needs to be identified. In theory, the more trees the better. However, based on results obtained for different number of trees ranging from 10 to 100 with an interval of 10 trees, the improvement of prediction accuracy with more trees is negligible (less than 0.1 %). Therefore, the number of trees is set to 10.

**Figure captions**

Figure 1. Schematic drawing of experimental setup (not to scale) and detailed view of the sensor array (in the duct).

Figure 2. Signals for 11 selected sensors and pre-ignition condition for Exp 8.

Figure 3. Comparison of IAQ and VOCs signals for 3 different tests (Exp 8, 46, and 57).

Figure 4. Schematic of moving windows with window size, $W$, and its corresponding label (the two sliding windows are not to scale; $t_i$ and $t_{i+1}$ are 4 s apart).

Figure 5. Performance comparison for Exp 8 and Exp 46 on OE and OFE data.

Figure 6. Overall performance on normal/unattended cooking classification for 3 machine learning models with different moving window size on OE and OFE data.

Figures 7. Performance improvement using the proposed object-oriented approach.

Figure 8. Overall performance on stove type classification for the 3 machine learning models with different moving window size on OE and OG data.

Figure 9. Overall performance on food type classification for the 3 machine learning models with different moving window size on OE and OFE data.